Response to Reviewers

26/10/20

Response to Reviewers of 1st revision of:

Rainforest-like Atmospheric Oxidation Pathways in a Polluted Megacity by Newland et al., 2020, submitted to ACP

General Response

We thank the editor and reviewers for giving up more of their time to make further insightful comments, helping to clarify and further improve our manuscript. The editor and reviewers recognise the importance of the results presented, and recommend publication in ACP after some minor changes. All changes to the manuscript are in line with the editor's and reviewers' comments and suggestions.

Responses to the editor and to each reviewer are given below. Responses to specific points raised by each reviewer are given separately beneath that point. Reviewers' comments are bold and italic, the authors' comments are inset in plain type.

Editor's Comments

Received and published: 26 September 2020

General Comments

1. Like reviewer 2, I am not convinced that these are "rainforest-like" conditions. The work describes a missing sink of NO that does not appear to produce ozone (similar to the Hofzumahaus publication referenced in the manuscript and as you point out). This means that the low NO has an unknown cause. This unknown chemistry puts in question whether the chemical regime is the same as in rainforests, or are the authors implying that the same unknown chemistry to keep NO low is active there. Figure 3 also is not very convincing for the conditions in Beijing from this work to be similar to those of Borneo and the rural SE-USA, although they are clearly different than London or NY. I think a clarification would be useful.

> Since this still appears to be confusing matters, we are happy to modify the title further to, '***Low NO Atmospheric Oxidation Pathways in a Polluted Megacity'.*** We think that subsequent references to 'rainforest-like' in the text are hopefully acceptable, and when mentioned that it is clear that we are referring to either the fact that there is low NO, or that the products observed are the same as those observed in VOC oxidation in a rainforest. E.g. we clarify this in the abstract saying that '… we observe significant formation of gas and aerosol phase oxidation products associated with the low-NO 'rainforest-like' regime…', highlighting that the reference to 'rainforest-like' refers to the mixing ratio of NO. We are not implying that the reason for the low NO is similar to the reason for low NO in a rainforest.

2. Unless I missed it, the manuscript does not comment on uncertainty or variability of measurements, with the exception of figure 4. Therefore, it is not possible to draw conclusions on whether there are statistically significant differences. Calibrations are only mentioned very briefly. For example, in figure S5 that one of the reviewer 2 comments one, it is not clear whether there are statistically significant differences or not. Uncertainty and variability should be considered in comparisons.

We have created a version of Figure 2 that shows the standard deviation of the mean for the diurnals. (These are not shown for the particle phase measurements as they are only from one day). We think that, while it is of course useful to show the variability in the data, adding the uncertainty makes the diurnal trends shown in Figure 2 more difficult to discern due to the necessity of extending the y-axis. Therefore, we have placed the figure with the standard deviations shown in the Supplementary Information as Figure S3, with a note added at the end of the first sentence in the caption of Figure 2 (below). If the editor considers that these should be shown on Figure 2 in the main manuscript then we could do this but may have to redesign the figure a little, changing the dimensions to make it higher and less wide.

> *Mean diurnal variation of measured organic and inorganic species in the gas phase and aerosol during the Beijing summer observations (data is filtered to only include 'typical' chemistry days – see text for details; the standard deviation of the mean is shown in Figure S3).*

CIMS: The calibration uncertainty on the CIMS measurements of IEPOX+ISOPOOH and ISOPONO2 is estimated at 50% based on the calibration using a standard for IEPOX. A further sentence to this effect has been added at the end of the CIMS part of the Methods section:

> *Absolute measurement uncertainties are estimated at 50% for the presented IEPOX+ISOPOOH and ISOPONO2 ($C_5H_9NO_4$) signals.*

PTR: The calibration uncertainty on the PTR measurements of m/z 71.05 has been estimated to be 21% using a transmission curve (Taipale et al., 2008). A further sentence to this effect has been added at the end of the PTR part of the Methods section:

> *The sensitivity for each mass was then calculated using a transmission curve. The maximum relative error for PTR-MS calibration using a relative transmission curve has been estimated to be 21% (Taipale et al., 2008).*

3. Similarly, the abstract has the statement "significant formation of gas and aerosol phase oxidation products associated with the low-NO 'rainforest like' regime". The word significance should be replaced with a quantitative number as it is not clear what significant means here. Are the amounts of ISOPOOH and IEPOX that are observed significant and what are they significant for? Similarly, are 20 ng/m3 of 2-MT-OS significant? The manuscript does not discuss how much overall SOA was observed and how much of it was from low-NO pathways, so the statement that there is significant formation of aerosol phase oxidation products is hard to evaluate.

The significance of the formation of the low NO products is that they demonstrate that low NO pathways are active. However, we acknowledge that we are not using the word *significant* here in a numerical sense and so have removed it. The significance in a more numerical sense is given a couple of sentences later in the abstract in the numbers from the modelling, i.e. that up to ~ 30 % of RO_2 are following low NO pathways in the afternoon.

The mean concentration of 2-MT-OS (11.8 ng m^{-3}) is of course lower than observed in the Amazon and SE US, but reaches up to a maximum of 100 ng m^{-3} or 1.2 % of the OOA measured by AMS (Bryant et al.,2020). In previous campaigns, mean 2-MT-OS mass concentrations were 83(wet)/399(dry) ng m^{-3} in the Amazon (Glasius et al., 2018), 169.5 ng m^{-3} in the SE USA (Budisulistiorini et al., 2015) and 5.3 ng m^{-3} in rural China, near Beijing (He et al., 2018). There is a lack of quantified data from other cities for comparison and so future work is needed to compare the importance of low NO oxidation pathways in cities where NO mixing ratios are higher.

In addition, recent studies indicate that 2-MT-OS may undergo further heterogeneous oxidation in highly oxidative environments such as Beijing, and so this is likely to be a lower limit for the amount that has actually formed through this pathway.

In this study we are using the IEPOX and 2-MT-OS data to show that low NO pathways can form SOA in Beijing. This is further evidenced by the observation of HOMs in the afternoon in Beijing by Brean et al. (2019) – already referenced in the manuscript. Furthermore, positive matrix factorisation of FIGAERO-CIMS data during the same campaign produced a factor that peaked in the afternoon (PM-OOA2) and had a large contribution from HOMs and isoprene oxidation products (Mehra et al. 2020; Faraday Discuss.). However, at this point much more research is needed to be able to determine the % of SOA forming from low NO chemistry.

Bryant, D. J., Dixon, W. J., Hopkins, J. R., Dunmore, R. E., Pereira, K. L., Shaw, M., Squires, F. A., Bannan, T. J., Mehra, A., Worrall, S. D., Bacak, A., Coe, H., Percival, C. J., Whalley, L. K., Heard, D. E., Slater, E. J., Ouyang, B., Cui, T., Surratt, J. D., Liu, D., Shi, Z., Harrison, R., Sun, Y., Xu, W., Lewis, A. C., Lee, J. D., Rickard, A. R., and Hamilton, J. F.: Strong anthropogenic control of secondary organic aerosol formation from isoprene in Beijing, Atmos. Chem. Phys., 20, 7531–7552, https://doi.org/10.5194/acp-20-7531-2020, 2020.

Glasius, M., Bering, M. S., Yee, L. D., De Sá, S. S., Isaacman-VanWertz, G., Wernis, R. A., Barbosa, H. M. J., Alexander, M. L., Palm, B. B., Hu, W., Campuzano-Jost, P., Day, D. A., Jimenez, J. L., Shrivastava, M., Martin, S. T., and Goldstein, A. H.: Organosulfates in aerosols downwind of an urban region in central Amazon, Environ. Sci. Process. Impact., 20, 1546–1558, https://doi.org/10.1039/c8em00413g, 2018.

He, Q. -F., Ding, X., Fu, X. -X., Zhang, Y. -Q., Wang, J. -Q., Liu, Y. -X., Tang, M. -J., Wang, X. -M., and Rudich, Y.: Secondary Organic Aerosol Formation From Isoprene Epoxides in the Pearl River Delta, South China: IEPOX- and HMML- Derived Tracers, J. Geophys. Res.-Atmos., 123, 6999–7012, https://doi.org/10.1029/2017JD028242, 2018.

Budisulistiorini, S. H., Li, X., Bairai, S. T., Renfro, J., Liu, Y., Liu, Y. J., McKinney, K. A., Martin, S. T., McNeill, V. F., Pye, H. O. T., Nenes, A., Neff, M. E., Stone, E. A., Mueller, S., Knote, C., Shaw, S. L., Zhang, Z., Gold, A., and Surratt, J. D.: Examining the effects of anthropogenic emissions on isoprene- derived secondary organic aerosol formation during the 2013 Southern Oxidant and Aerosol Study (SOAS) at the Look Rock, Tennessee ground site, Atmos. Chem. Phys., 15, 8871–8888, https://doi.org/10.5194/acp-15-8871-2015, 2015.

4. According to Nguyen et al. (PCCP 17, 17914-17926, 2015) MPAN produces SOA via oxidation by OH to form HMML without any participation NO or HO2, so it would be useful if the authors could explain how SOA from MPAN indicates low NO conditions.

The formation of 2-MGA-OS requires high and then low NO conditions (in fact not necessarily low NO but a low NO/NO_2 ratio). MACR is formed (predominantly) from oxidation of isoprene in a high NO environment. Then the afternoon low NO/NO_2 ratio leads to efficient formation of MPAN from OH initiated MACR oxidation and subsequent oxidation to 2-MGA via HMML.

We have clarified this in the text changing it from:

> *Both are tracers for low-NO chemistry, with 2-methyltetrol-OS formed via the low HO2 IEPOX pathway (Paulot et al., 2009; Surratt et al., 2010; Lin et al., 2012), while 2-MGA-OS (Lin et al., 2013) is formed from the oxidation of MPAN (Kjaergaard et al., 2012; Nguyen et al., 2015), itself formed from the high-NO isoprene oxidation product MACR, in an environment with a high NO2/NO ratio, as seen in the afternoon in Beijing, and further oxidation leads to 2-MGA (Surratt et al., 2010; Chan et al., 2010; Nguyen et al., 2015).*

To:

> *Both are tracers for non-NO RO_2 chemistry. While 2-methyltetrol-OS is formed via the ISOPOO+HO_2 IEPOX pathway (Paulot et al., 2009; Surratt et al., 2010; Lin et al., 2012), 2-MGA-OS (Lin et al., 2013) is formed from the OH initiated oxidation of MPAN (Kjaergaard et al., 2012; Nguyen et al., 2015), with further oxidation leading to 2-MGA (Surratt et al., 2010; Chan et al., 2010; Nguyen et al., 2015). MPAN is a product of the OH initiated oxidation of MACR in an environment with a high NO_2/NO ratio. So the observation of 2-MGA-OS formation reflects the observed diurnal NO cycle in Beijing. MACR is formed in the morning through the OH oxidation of isoprene in a high NO environment, followed by OH oxidation of MACR in a high NO_2/NO environment in the afternoon to form MPAN, which reacts further with OH to yield 2-MGA.*

5. Lastly, it would be useful to comment on HO2 measurements, which LIF FAGE instruments often measure, as a comparison could help evaluate the fNO number as it in large part depends on competition between NO and HO2.

The HO_2 measurements from the campaign are now available in Whalley et al. (2020) (doi: 10.5194/acp-2020-785). The mean diurnal [HO_2] for the campaign peaks in the mid-afternoon with a campaign mean for the daily peak of roughly $5x10^8$ cm^{-3}, although on some days this is as high as $8x10^8$ cm^{-3}. With NO falling to < 1 ppb on most days in the afternoon, and sometimes to < 100 ppt, the calculated contribution of the low NO pathway is in the range of 10 – 50 %, as borne out by the model. We have included the following in the discussion in Section 3: Box Modelling.

HO_2 concentrations were measured by FAGE during the campaign (Whalley et al., 2020). Concentrations peaked in mid-afternoon (i.e. when NO is at its lowest), regularly exceeding 5 × 10^8 cm^{-3} and reaching up to 1 × 10^9 cm^{-3} on some days. Based on the relative reaction rates of RO_2 with NO and HO_2, for $[HO_2]$ = 5 × 10^8 cm^{-3} the contribution of low NO pathways to RO_2 removal would be expected to be roughly 50 % at [NO] = 100 ppt and 10 % at [NO] = 1 ppb.

Box modeling using the MCM and constraining to the measurements from Beijing in Whalley et al. (2020) (similar to that done in this paper) tends to over-predict the HO_2 concentrations measured by the FAGE. One solution put forward by Whalley et al. that can greatly improve model-measurement comparison of $[HO_2]$ is the inclusion of some parameterised HOMs / auto-oxidation chemistry, in which RO_2+NO leads to further RO_2 rather than to HO_2. This effectively increases the number of RO_2+NO reactions per HO_2 formed. This would also qualitatively fit with our observation of a missing NO sink. It is now well recognised that the current generation of semi-explicit chemical mechanisms (e.g. MCMv3.3.1) are missing much of this auto-oxidation, H-shift chemistry and this is one of the main foci in developing new generations of such mechanisms. This is even more the case for the reduced mechanisms included in global models such as GEOS-Chem. We have already touched on this in the discussion as a possible explanation for the inability of GEOS-Chem to replicate the observed diurnal cycle of NO. We have now expanded this discussion slightly.

This paragraph has changed from:

The fact that the GEOS-Chem modelling cannot recreate the extremely low afternoon NO suggests that there may be additional sinks for NO beyond our current chemical understanding. One explanation may be additional NO sinks that recycle OH without producing O_3, as previously proposed for the high VOC-low NO (< 1ppbv) conditions seen in Beijing and other cities (Hofzumahaus et al., 2009; Whalley et al., 2018; Tan et al., 2019). Another explanation may be the presence of high concentrations of other species that can rapidly convert NO to NO_2 e.g. halogen oxides.

To:

The fact that the GEOS-Chem modelling cannot recreate the extremely low NO levels observed in the afternoon suggests that there may be additional sinks for NO beyond those currently included in the chemical mechanism. One explanation may be the occurrence of RO_2+NO oxidation pathways that lead to the formation of a second RO_2 before forming a stable species, effectively increasing the efficiency of NO to NO_2 conversion per initial oxidation step (e.g. Whalley et al., 2020). Such reactions are expected to be particularly important for larger and more complex VOCs, for which the detailed oxidation processes have been less studied and which are heavily parameterised in global models. Auto-oxidation processes that regenerate OH, leading to the formation of further RO_2 have also been proposed previously for the high VOC-low NO (< 1ppbv) conditions seen in Beijing and other cities (Hofzumahaus et al., 2009; Whalley et al., 2018; Tan et al., 2019). Inclusion of such novel RO_2 oxidation processes is one of the main foci of the next generation of atmospheric chemical mechanisms. Another explanation may be the presence of

high concentrations of other species (not currently included in the chemical scheme) that can rapidly convert NO to NO_2, e.g. halogen oxides.

Whalley, L. K., Slater, E. J., Woodward-Massey, R., Ye, C., Lee, J. D., Squires, F., Hopkins, J. R., Dunmore, R. E., Shaw, M., Hamilton, J. F., Lewis, A. C., Mehra, A., Worrall, S. D., Bacak, A., Bannan, T. J., Coe, H., Ouyang, B., Jones, R. L., Crilley, L. R., Kramer, L. J., Bloss, W. J., Vu, T., Kotthaus, S., Grimmond, S., Sun, Y., Xu, W., Yue, S., Ren, L., Acton, W. J. F., Hewitt, C. N., Wang, X., Fu, P., and Heard, D. E.: Evaluating the sensitivity of radical chemistry and ozone formation to ambient VOCs and NO_x in Beijing, Atmos. Chem. Phys. Discuss., https://doi.org/10.5194/acp-2020-785, in review, 2020.

Anonymous Referee #1

Received and published: 20 July 2020

The aim of the revised manuscript by Newland et al. is now tightly focused on the key, high impact result: The authors use isoprene oxidation products as photochemical markers of the changing chemical pathways throughout the daytime and demonstrate that the model used to capture this diurnal change fail.

Figure 4 shows that measured NO is high in the morning and low in the afternoon. It is not surprising that isoprene oxidation forms typically high NO products in the morning and low NO products in the afternoon.

We agree that, on the face of it this is not surprising, but this is exactly the point of this Letter, the suite of gas and aerosol phase product observations corroborate the observed diurnal suppression of NO and highlight the effects of this chemical cycle – i.e. the production of OVOC / SOA products that are associated with low-NO chemistry and are not typically expected to be found in a highly polluted urban environment.

At low NO, RO2 radicals especially ISOPOO are reacting with HO2 and RO2 rather than with NO. In Beijing the complex VOC composition leads to a complex mixture of RO2 radicals. The reaction between these RO2 radicals might be the key to get a better match with measurements when included in models.

Yes, we agree that this is what is happening. Although RO_2+RO_2 reactions are likely to be negligible since [RO_2] are likely to be lower than [HO_2] and $k_{HO2+RO2}$ is generally at least two orders of magnitude greater than $k_{RO2+RO2}$ (though there may be some surprisingly fast RO_2 cross reaction rates - and this is certainly an area that requires further research at a laboratory kinetics level).

The authors explicitly deny to describe the VOC composition in Beijing, talk about the role of isoprene chemistry in Beijing, or talk about ozone production in Beijing.

Therefore I question the key, high impact of the result presented here.

As highlighted in the previous response, this discussion is out of scope of this highly focused Letter, but is important and the subject of other publications led by some of the co-authors (which have in the meantime been published). Further details of these points are now available in Whalley et al. (2020) (doi: 10.5194/acp-2020-785). We maintain that, while these are undoubtedly of interest scientifically, they are not relevant to the message of this Letter.

As explained in the next paragraph measured PTR-MS signal at 71.05 m/z cannot be assigned quantitatively to MVK+MACR. The new Figure S5, thought to support MVK+MACR assignment of signal at 71.05 m/z, is misinterpreted.

Fig. S5 demonstrates that there is agreement between the PTR-MS signal at 71.05 m/z measured in the morning from 7:00 to 11:00 comparing different inlet lines. But there is a striking difference in the afternoon. From 16:00 to 18:00 both lines taking air at 102 m show 0.8 ppb (flux line, PFA, transport time 68 s) vs. < 0.6 ppb (gradient line, sample being drawn into stainless steel containers).

We think that the reviewer has misinterpreted which line refers to which sampling method in Figure S5. The deviation at 17:00 is between the two gradient sampling lines and the flux line (rather than the two methods sampling from 102 m and that from 3 m as suggested by the reviewer).

In the morning when high NO isoprene chemistry produces prevailingly MVK + MACR that is detected at 71.05 m/z the agreement between the two inlet lines from the same intake point is reasonable. In the afternoon under low NO, MVK, MACR, ISOPOOH and IEPOX is formed contributing with different sensitivities to the 71.05 m/z PTR signal.

All PTR-MS data and discussion termed MVK+MACR have to be taken out from the manuscript.

See comment on Figure 2f below. The line where MACR+MVK is first mentioned has been changed from:

> *The profile of the high-NO products MACR+MVK, measured by Proton Transfer Reaction Time-of-Flight Mass Spectrometer (PTR-ToF-MS) – see Methods for further details, is very similar to that of $ISOPONO_2$ until about 15:00, when they begin to increase, with a second peak observed at around 17:00 (Figure 2f).*

To:

> *The profile of the signal at m/z 71.05 is assumed to be dominated by the high-NO products MACR+MVK, measured by Proton Transfer Reaction Time-of-Flight Mass Spectrometer (PTR-ToF-MS) – see Methods for further details. This signal is very similar to that of $ISOPONO_2$ until about 15:00, when it begins to increase, with a second peak observed at around 17:00 (Figure 2f).*

Line 587: The PTR-TOF-MS signal at 71.05 m/z is not MVK+MACR. Fig. S5 demonstrates that different inlet lines lead to strongly different signal intensities erroneously termed MVK+MACR.

It is unclear how the reviewer interprets Figure S5 as demonstrating strongly different signal intensities.

Line 590: 1,2-ISOPOOH, which is mainly produced in isoprene OH reactions converts at stainless steel surfaces to MVK.

The reviewer makes a good point, this sentence has been changed from:

> *This latter peak may be an observational artefact as a result of the conversion of ISOPOOH to MACR on metal surfaces within the inlet of the PTR instrument (Rivera-Rios et al., 2014).*

To:

This latter peak may be an observational artefact as a result of the conversion of ISOPOOH to either MVK (via 1,2-ISOPOOH - the dominant isomer (Reeves et al., 2020)) or MACR (via 4,3-ISOPOOH) on metal surfaces within the inlet of the PTR instrument (Rivera-Rios et al., 2014).

Reeves, C. E., et al.: Observations of speciated isoprene nitrates in Beijing: implications for isoprene chemistry, Atmos. Chem. Phys. Discuss., https://doi.org/10.5194/acp-2019-964, in review, 2020.

Figure 2f: The assignment of the signal at 71.05 m/z as MVK+MACR is not correct. Figure 2f has to be taken out.

Figure 2f has not been taken out, but the axis has been changed to m/z 71.05 rather than MACR+MVK. Thus readers can see in the text and the figure caption the discussion of the attribution of m/z 71.05 to MACR+MVK or potentially to other sources such as ISOPOOH. The following has been added to the figure caption:

(f) m/z 71.05, assumed to be predominantly the gas phase isoprene 'high NO' oxidation products methacrolein (MACR) (precursor to 2-MGA) + methyl vinyl ketone (MVK), signal calibrated with MACR/MVK – see text for further details.

The new title "Rainforest-like Atmospheric Oxidation Pathways in a Polluted Megacity" is misleading because: The key result here is connected with changing chemical pathways throughout the daytime due to NO availability. There is not such a NO change in the rainforest! The VOC composition and reactivity is also very much different in the rainforest. Therefore I suggest to take out the word "rainforest" from the title, which is misleading.

The word rainforest has now been removed from the title – see reply to the editor's comment for further detail.

Anonymous Referee #2

Received and published: 08 July 2020

The revisions made in the previous review stage are sufficient for publication with one minor update:

Figure 4: In the previous submission the ozone observations agreed with the model results quite well. However, in the updated version of the manuscript, ozone is not represented well by the model contrary to what is stated in the text. It is important to note that the model under-predicts ozone in the mean (particularly in the afternoon) and the spread (if I interpret the shading correctly?) is also very different with the high ozone days in the observations clearly missed within the model. To make this point clearer, please specify in the figure 4 caption what the shading represents? Is this the 25th to 75th percentile? With this updated figure, it appears that the model's inability to represent the low NO values is potentially connected with not representing the high ozone events correctly and this should be noted in the text.

The shaded areas represent +/- two standard deviations of the mean of the diurnals. This has now been noted in the figure caption.

The reviewer is correct that the model under-predicts the measured ozone diurnal peak by about 10 % (this is a little less than in the previous version of the figure – see comments below for further details on slight changes to the way the figure has been presented). This has now been noted in the Discussion section (below). But also noted is that this slight under-prediction of ozone cannot be responsible for the overprediction of [NO], which is over-predicted in the afternoon by a factor of 3 – 5.

> *The mean afternoon ozone peak is under-predicted by the model by about 10 %. However, this has little impact on the modelled NO concentrations which the model over-predicts by a factor of 3 - 5 through the afternoon.*

The GEOS-Chem modelling presented in the supplement of the original version of the manuscript was compared to diurnals calculated using the full measurement dataset from the campaign (not the filtered data presented in Figure 2). For the revised version of the manuscript, in which the GEOS-Chem modelling became Figure 4, we realised that we were now presenting different measurement data for NO_x and O_3 in Figure 4 compared to Figure 2 (the diurnal means of the full campaign compared to the diurnal means of the filtered data). We felt that we should present the same measurements in both plots so this now compared the diurnals calculated using the filtered data to modelled diurnals for the whole campaign. (Ideally, we would perform the GEOS-Chem modelling with the filtered days removed. However, it is not apparently possible to simply filter out days for the GEOS-Chem modelling). This meant that the modelling was now somewhat underpredicting the ozone compared to the measurements (as low ozone days are filtered out of the measurements).

In addition, the GEOS-Chem modelling in the original manuscript scaled isoprene emissions regionally, whereas the modelling in the revised version scaled the isoprene emissions locally over the Beijing urban area. This had a small effect on modelled ozone, reducing the modelled diurnal peak by about 10 %.

We now present the modelling using the locally scaled isoprene emissions, and compare to the diurnals calculated from the full measurement dataset. This is now noted in the figure caption and in the text. A line has also been added about the scaling of isoprene emissions at the end of the GEOS-Chem modeling description in Methods.

> *Isoprene emissions calculated by the MEGAN biogenic emissions extension were scaled by 2.5x in the Beijing metropolitan region (Jing-Jin-Ji).*

None of this changes the general conclusion that the GEOS-Chem model is unable to recreate the observed diurnal NO cycle. And this is the case whether the filtered or unfiltered dataset is used.

Marked-up
Manuscript Version

Low NO Atmospheric Oxidation Pathways in a Polluted Megacity

Mike J. Newland[1], Daniel J. Bryant[1], Rachel E. Dunmore[1], Thomas J. Bannan[2], W. Joe F. Acton[3], Ben Langford[4], James R. Hopkins[1,5], Freya A. Squires[1], William Dixon[1], William S. Drysdale[1], Peter D. Ivatt[1], Mathew J. Evans[1], Peter M. Edwards[1], Lisa K. Whalley[6,7], Dwayne E. Heard[6,7], Eloise J. Slater[6], Robert Woodward-Massey[8], Chunxiang Ye[8], Archit Mehra[2], Stephen D. Worrall[2,a], Asan Bacak[2], Hugh Coe[2], Carl J. Percival[2,b], C. Nicholas Hewitt[3], James D. Lee[1,5], Tianqu Cui[9], Jason D. Surratt[9], Xinming Wang[10], Alastair C. Lewis[1,5], Andrew R. Rickard[1,5], Jacqueline F. Hamilton[1]

[1]Wolfson Atmospheric Chemistry Laboratories, Department of Chemistry, University of York, York, UK
[2]School of Earth and Environmental Sciences, The University of Manchester, Manchester, UK
[3]Lancaster Environment Centre, Lancaster University, Lancaster, UK
[4]Centre for Ecology and Hydrology, Edinburgh, EH26 0QB, UK
[5]National Centre for Atmospheric Science (NCAS), University of York, York, UK
[6]School of Chemistry, University of Leeds, Leeds, UK
[7]National Centre for Atmospheric Science, School of Chemistry, University of Leeds, UK
[8]Beijing Innovation Center for Engineering Science and Advanced Technology, State Key Joint Laboratory for Environmental Simulation and Pollution Control, Center for Environment and Health, College of Environmental Sciences and Engineering, Peking University, Beijing, 100871, China
[9]Department of Environmental Sciences and Engineering, Gillings School of Global Health, University of North Carolina, Chapel Hill, USA
School of Engineering and Applied Science, Aston University, Birmingham, UK
[10]Guangzhou Institute of Geochemistry, Chinese Academy of Sciences, Guangzhou, China
[a]now at: Chemical Engineering and Applied Chemistry, School of Engineering and Applied Science, Aston University, Birmingham, UK
[b]now at: Jet Propulsion Laboratory, California Institute of Technology, 4800 Oak Grove Drive, Pasadena, CA, USA

Correspondence to: Mike J. Newland (mike.newland@york.ac.uk)
Jacqueline F. Hamilton (Jacqui.hamilton@york.ac.uk)

Abstract. The impact of volatile organic compound (VOC) emissions to the atmosphere on the production of secondary pollutants, such as ozone and secondary organic aerosol (SOA), is mediated by the concentration of nitric oxide (NO). Polluted urban atmospheres are typically considered to be "high-NO" environments, while remote regions such as rainforests, with minimal anthropogenic influences, are considered to be "low-NO". However, our observations from central Beijing show that this simplistic separation of regimes is flawed. Despite being in one of the largest megacities in the world, we observe formation of gas and aerosol phase oxidation products usually associated with low-NO 'rainforest-like'

Deleted: Rainforest-likeLow NO

Deleted: significant

Deleted: the

atmospheric oxidation pathways during the afternoon, caused by extreme suppression of NO concentrations in the afternoon. Box model calculations suggest that during the morning high-NO chemistry predominates (95%) but in the afternoon low-NO chemistry plays a greater role (30%). Current emissions inventories are applied in the GEOS-Chem model which shows that such models, when run at the regional scale, fail to accurately predict such an extreme diurnal cycle in the NO concentration. With increasing global emphasis on reducing air pollution, it is crucial for the modelling tools used to develop urban air quality policy to be able to accurately represent such extreme diurnal variations in NO to accurately predict the formation of pollutants such as SOA and ozone.

Deleted: regime

Deleted: run

1 Introduction

The atmosphere in polluted urban areas has a markedly different chemical composition to that in remote regions (e.g. rainforests). This can lead to changes in the chemical oxidation pathways for volatile organic compounds (VOCs), giving rise to the formation of different secondary pollutants. Oxidation by hydroxyl radicals (OH) is the dominant daytime sink for VOCs, leading to the formation of highly reactive peroxy radicals (RO_2). In atmospheres with high concentrations of nitric oxide (NO), emitted by combustion sources such as vehicles, cooking, and energy generation, RO_2 radicals react predominantly with NO (Orlando and Tyndall, 2012). This tends to break the initial VOC down to smaller, more oxidised VOCs, and can also produce organic nitrates ($RONO_2$). This pathway also produces NO_2, the photolysis of which leads to ozone production. In contrast, in low-NO atmospheres RO_2 predominantly react with other RO_2, including hydroperoxyl radicals (HO_2), or can isomerize/auto-oxidise to form different multi-functionalized oxygenated RO_2 (Crounse et al., 2013). These low NO pathways tend to maintain the original carbon skeleton. The large highly oxidised molecules formed can efficiently partition to the aerosol phase to yield secondary organic aerosol (SOA) (Bianchi et al., 2019), which often comprises a large fraction of submicron atmospheric particulate matter (PM) in many regions (Jimenez et al., 2009).

In the past twenty years, emissions, and hence atmospheric concentrations, of nitrogen oxides (NO_x) have decreased in urban areas throughout the majority of the developed world. In urban areas this has been due to improvements in vehicle emissions technologies, changes to residential heating, and in many major

European cities, due to restrictions on the types of vehicles that are allowed in certain areas at certain times of the day. In China, through the introduction of the "Air Pollution Prevention and Control Action Plan" in 2013 (Zhang et al. 2019) there has been a concerted effort to reduce pollutant emissions. Numerous pollution control measures have been introduced, including: improved industrial emissions standards; the promotion of clean fuels instead of coal within the residential sector; improving vehicle emissions standards; and taking older vehicles off the road. In Beijing, 900,000 households have converted from using coal to cleaner technologies such as gas or electricity since 2013. These actions have led to a 32 % decrease in NO_2 emissions since 2012 (Liu et al., 2016; Krotkov et al., 2016; Miyazaki et al., 2017). Most significant for NO_x emissions however is the stringent vehicle control measures introduced within the last decade, accounting for 47 % of the total reduction in emissions for the city (Cheng et al. 2019). Such reductions in NO_x emissions are expected to lead to an increased importance of low-NO oxidation pathways for VOCs in urban and suburban areas (e.g. Praske et al., 2018). This will lead to the production of a range of low volatility multi-functionalised products, efficient at producing SOA, which have previously been found only in remote environments removed from anthropogenic influence.

Surface ozone in Beijing has increased through the 1990s and 2000s (Tang et al., 2009). The city regularly experiences daily peaks in the summer-time of over 100 ppb (e.g. Wang et al., 2015). Such high ozone episodes are a function both of chemistry and meteorology, with air masses coming from the mountainous regions to the northwest tending to bring in clean air low in ozone, while air masses coming from the densely populated regions to the south and west bring processed polluted air high in ozone (Wang et al., 2017). A number of modelling studies have concluded that the sources of the ozone during high ozone episodes are a combination of both local production and regional transport (Wang et al., 2017; Liu et al., 2019).

Biogenic sources dominate global emissions of VOCs to the atmosphere, with the highly reactive VOC isoprene (2-methyl-1,3-butadiene) contributing ~70% by mass (Sindelarova et al., 2014). The gas and aerosol phase products of isoprene oxidation have been extensively characterized in the laboratory

(Wennberg et al., 2018, and references therein). For isoprene, the low-NO oxidation pathway leads to low volatility products, such as isoprene hydroperoxides (ISOPOOH), that can go on to form significant quantities of SOA via formation of isoprene epoxides (IEPOX) (Figure 1) (Paulot et al., 2009; Surratt et al., 2010; Lin et al., 2012). The high-NO pathway can also form SOA via the formation of methacrolein (MACR), which can react further to form SOA constituents such as 2-methylglyceric acid (2-MGA) and corresponding oligomers (Kroll et al., 2006; Surratt et al., 2006; 2010; Nguyen et al., 2015) (Figure 1). Other significant contributors to isoprene-SOA formed via the high NO pathway include nitrates (e.g. $ISOPONO_2$) and dinitrates (Schwantes et al., 2019). In this work, a suite of isoprene oxidation products, in both the gas and particle phases, are used as tracers of the changing atmospheric chemical environment through the daytime in Beijing.

2 Results

Beijing is a megacity (population of 21.4 M) with an atmospheric reactive VOC mix with both biogenic and anthropogenic influences (e.g. Li et al., 2020). Mean diurnal cycles of ozone, NO, isoprene, and a range of gas and aerosol phase isoprene oxidation products measured at a city-centre site in summer 2017 (Shi et al., 2019) are shown in Figure 2. Data is filtered to only include 'typical' chemistry days, which are considered to be when the ozone mixing ratio increases through the morning to an afternoon peak of > 70 ppb. Such 'typical' days account for 25 of the total of 34 measurement days. Further details of the data filtering is given in Section S1 of the Supplementary Information. Ozone increases throughout the day to a mid-afternoon peak (Figure 2a), driven by the photolysis of NO_2, which is rapidly regenerated through the reactions of ozone, RO_2 and HO_2 with NO. The high level of ozone acts to suppress NO concentrations. Such a diurnal cycle is typical of urban environments (Ren et al., 2003; Whalley et al., 2018). However, ozone is so high in Beijing, with mixing ratios regularly >100 ppbv in the afternoon, that on many days NO concentrations fall to < 0.5 ppbv in the afternoon, and on some days to < 0.1 ppbv (see Figure S4&5).

Deleted: S2

The observed diurnal cycles of 'low-NO' and 'high-NO' isoprene oxidation products (Figure 1) in both the gas and aerosol phases can be explained by the observed diurnal cycle of NO (Figure 2c). The high-

NO product isoprene nitrate ($ISOPONO_2$), measured using a Chemical Ionisation Mass Spectrometer (CIMS) – see Methods for further details, is produced through the morning from reaction of isoprene peroxy radicals (ISOPOO) with NO (Figure 2d). During the afternoon, an increasing fraction of ISOPOO begins to react with HO_2 or RO_2 as the NO concentration drops. This leads to the observed decrease in $ISOPONO_2$, and an increase in the low-NO products IEPOX + ISOPOOH (also measured by CIMS) through the afternoon (Figure 2e). The profile of the signal at m/z 71.05 is assumed to be dominated by the high-NO products MACR+MVK, measured by Proton Transfer Reaction Time-of-Flight Mass Spectrometer (PTR-ToF-MS) – see Methods for further details. This signal is very similar to that of $ISOPONO_2$ until about 15:00, when it begins to increase, with a second peak observed at around 17:00 (Figure 2f). This latter peak may be an observational artefact as a result of the conversion of ISOPOOH to either MVK (via 1,2-ISOPOOH - the dominant isomer (Reeves et al., 2020)) or MACR (via 4,3-ISOPOOH) on metal surfaces within the inlet of the PTR instrument (Rivera-Rios et al., 2014). Isoprene oxidation products can also partition into the particle phase and undergo heterogeneous reactions to form organosulfates, with concentrations driven by a number of additional factors such as particulate sulfate and water vapour concentrations. Isoprene organosulfate tracers, 2-MGA-OS (Figure 2g), and 2-methyltetrol-OS (Figure 2h), and were measured on 11 June, with low concentrations through the morning, increasing during the afternoon to a peak around 15:00-16:00. Both are tracers for non-NO driven chemistry. While 2-methyltetrol-OS is formed via the ISOPOO+HO_2 IEPOX pathway (Paulot et al., 2009; Surratt et al., 2010; Lin et al., 2012), 2-MGA-OS (Lin et al., 2013) is formed from the OH initiated oxidation of MPAN (Kjaergaard et al., 2012; Nguyen et al., 2015), with further oxidation leading to 2-MGA (Surratt et al., 2010; Chan et al., 2010; Nguyen et al., 2015). MPAN is a product of the OH initiated oxidation of MACR in an environment with a high NO_2/NO ratio. So the observation of 2-MGA-OS formation reflects the observed diurnal NO cycle in Beijing. MACR is formed in the morning through the OH oxidation of isoprene in a high NO environment, followed by OH oxidation of MACR in a high NO_2/NO environment in the afternoon to form MPAN, which reacts further with OH to yield 2-MGA.

Deleted: ,

Deleted: they

Deleted: This latter peak may be an observational artefact as a result of the conversion of ISOPOOH to MACR on metal surfaces within the inlet of the PTR instrument (Rivera-Rios et al., 2014).

Deleted: Organosulfate

Formatted: Font: Not Italic

Deleted: Both are tracers for low-NO chemistry, with 2-methyltetrol-OS formed via the low HO_2 IEPOX pathway (Paulot et al., 2009; Surratt et al., 2010; Lin et al., 2012), while 2-MGA-OS (Lin et al., 2013) is formed from the oxidation of MPAN (Kjaergaard et al., 2012; Nguyen et al., 2015), itself formed from the high-NO isoprene oxidation product MACR, in an environment with a high NO_2/NO ratio, as seen in the afternoon in Beijing, and further oxidation leads to 2-MGA (Surratt et al., 2010; Chan et al., 2010; Nguyen et al., 2015).

The observed temporal profiles of the isoprene tracer products suggest a chemical cycle switching from a high-NO to a low-NO chemical regime during the day in Beijing. First, isoprene nitrates, formed predominantly during the morning (Figure 2d), are characteristic of high-NO chemistry. Second, isoprene hydroperoxides (ISOPOOH) and epoxydiols (IEPOX) (Figure 2e), formed predominantly during the afternoon, are characteristic of low-NO chemistry, where the reaction of ISOPOO with HO_2 dominates over reaction with NO. The formation of highly oxygenated molecules (HOMs), characteristic of RO_2 isomerisation and auto-oxidation in low NO environments, has also been observed during the afternoon at this site (Brean et al., 2019). Third, the observation of large amounts of 2-methylglyceric acid (2-MGA-OS) (Figure 2g) in the aerosol is suggestive of both high and low NO chemistry having occurred.

Deleted: b

3 Box Modelling

The chemical box model DSMACC (Emmerson and Evans, 2009), coupled with the near-explicit oxidation mechanism for isoprene from the Master Chemical Mechanism (MCM v3.3.1) (Jenkin et al., 1997; 2015), was used to assess the sensitivity of the fraction of ISOPOO reacting with NO (f_{NO}) to varying NO concentrations and OH reactivities ($\sum \boldsymbol{k_{OH+VOC}}$ [VOC]). The model was run to steady state at a range of different fixed concentrations of [OH], [NO], and [isoprene], using fixed photolysis rates typical of Beijing daytime (see Section Methods and Section S5 in Supplementary Information). Figure 3 shows that, as expected, f_{NO} increases with increasing NO concentration. It also shows that f_{NO} is not a fixed value for a given concentration of NO, but decreases with the increasing reactivity of the system (the x-axis in Figure 3). The reactivity varies as a function of the VOC mixing ratios, the reactivity of the VOCs, and the OH concentration, i.e. [OH] × OH reactivity* (Equation E1). Higher reactivity and higher OH concentrations both lead to a higher concentration of peroxy radicals ($[HO_2] + \sum[RO_2]$), reducing f_{NO}. Average measurements of ([OH] × OH reactivity*) and [NO] for the afternoon (12:00 – 20:00) from a range of different environments are shown in Figure 3 (see also Table S1). The RO_2 chemistry in the rural southeastern US and the Borneo rainforest lies in the low NO regime (i.e. $f_{NO} < 0.5$) for the whole afternoon. In the urban areas of London and New York the chemistry remains in the high NO regime through the whole afternoon. However, in Beijing, the extreme suppression of NO concentrations in the

afternoon drives the chemistry from a regime in which > 95 % of the RO_2 is reacting with NO during the morning, to one in which less than 70 % is reacting with NO by mid-afternoon. HO_2 concentrations were measured by FAGE during the campaign (Whalley et al., 2020). Concentrations peaked in mid-afternoon (i.e. when NO is at its lowest), regularly exceeding 5×10^8 cm^{-3} and reaching up to 1×10^9 cm^{-3} on some days. Based on the relative reaction rates of RO_2 with NO and HO_2, for $[HO_2] = 5 \times 10^8$ cm^{-3} the contribution of low NO pathways to RO_2 removal would be expected to be roughly 50 % at [NO] = 100 ppt and 10 % at [NO] = 1 ppb.

4 Discussion and Conclusions

Deleted: 5

Modelling was performed with the global chemical transport model GEOS-Chem, with a nested grid at 0.25 x 0.3125 degree resolution over China (see Methods – GEOS-Chem modelling), to investigate the modelled diurnal cycle of NO for Beijing. The results are compared to the measurements for the entire campaign (note not the filtered measurements presented in Figure 2) (Figure 4). These show that while the model does a good job of recreating the measured ozone and NO_2 diurnal profiles for the campaign period, it cannot match the observed diurnal profiles of [NO] or the NO to NO_2 ratio, particularly at sub ppb levels typically observed during the afternoon. Thus the model will not capture the formation of low NO products from isoprene and other VOCs in Beijing. The major driver of the low NO concentrations in the model is the high levels of ozone, which titrates out the NO. The mean afternoon ozone peak is under predicted by the model by about 10 %. However, this has little impact on the modelled NO concentrations which the model over predicts by a factor of 3 – 5 through the afternoon. As such, with the chemistry currently in the model there is very little flexibility available to appreciably change this ratio, i.e. changes to other NO sinks in the model, such as RO_2, through changes to VOC emissions, will have little effect on [NO]. The fact that the GEOS-Chem modelling cannot recreate the extremely low NO levels observed in the afternoon suggests that there may be additional sinks for NO beyond those currently included in the chemical mechanism. One explanation may be the occurrence of RO_2+NO oxidation pathways that lead to the formation of a second RO_2 before forming a stable species, effectively increasing the efficiency of NO to NO_2 conversion per initial oxidation step (e.g. Whalley et al., 2020).

Deleted: is unable to

Deleted:

Such reactions are expected to be particularly important for larger and more complex VOCs, for which the detailed oxidation processes have been less studied and which are heavily parameterised in global models. Auto-oxidation processes that regenerate OH, leading to the formation of further RO_2 have also been proposed previously for the high VOC-low NO (< 1ppbv) conditions seen in Beijing and other cities (Hofzumahaus et al., 2009; Whalley et al., 2018; Tan et al., 2019). Inclusion of such RO_2 oxidation processes is one of the main foci of the next generation of atmospheric chemical mechanisms. Another explanation may be the presence of high concentrations of other species (not currently included in the chemical scheme) that can rapidly convert NO to NO_2, e.g. halogen oxides.

Deleted: The fact that the GEOS-Chem modelling cannot recreate the extremely low afternoon NO suggests that there may be additional sinks for NO beyond our current chemical understanding. One explanation may be additional NO sinks that recycle OH without producing O_3, as previously proposed for the high VOC-low NO (< 1ppbv) conditions seen in Beijing and other cities (Hofzumahaus et al., 2009; Whalley et al., 2018;; 2020; Tan et al., 2019). Another explanation may be the presence of high concentrations of other species that can rapidly convert NO to NO_2 e.g. halogen oxides.

Similar mixed NO regimes as observed here for Beijing have been observed previously at a suburban site in the Pearl River Delta (Tan et al., 2019), and in the semi-rural south east US (Xiong et al., 2015), albeit with lower morning NO peaks. Such a mixed regime will lead to a range of low volatility multifunctional products (Xiong et al., 2015; Lee et al., 2016) some of which are only accessible through this regime, which can efficiently partition to the particle phase to contribute to SOA. With the rates of RO_2+NO, and RO_2+HO_2 similar for most peroxy radicals (Orlando and Tyndall, 2012), the chemical regime reported herein is not just relevant to isoprene, but to all VOCs (see a comparison for butane and toluene in the Supplementary Information Figure S11).

Our observations from Beijing challenge the commonly accepted view of polluted urban areas as high-NO atmospheric environments in two ways. First, very high ozone (and other sinks) regularly reduces afternoon NO to < 1 ppbv, and on some days to < 0.1 ppbv. This leads to the formation of 'low-NO' products in the gas and aerosol phase. Second, the level of NO that is required for 'low-NO chemistry' to occur is not a fixed value, but is dependent on the concentration and reactivity of the VOCs present and the concentration of OH. Hence NO concentrations that represent 'low-NO' conditions in a tropical rainforest, for example, are different to those that represent 'low-NO' conditions in a highly polluted urban environment with elevated VOC/OH reactivity.

Under the conditions observed in Beijing, the production of low-NO SOA and the associated increase in PM is shown to be closely linked to photochemical ozone production. Policies that reduce the afternoon

ozone peak might also be expected to reduce the production of these aerosol-phase products. However, such policies must also take account of the complex interactions between NO_x, VOCs, ozone, and PM. For example, reducing NO_x emissions can counter-intuitively lead to increases in ozone, as has occurred in other major cities (Air Quality Expert Group, 2009), while a recent modelling study (Li et al., 2019) has suggested that reducing PM has led to increases in ozone in China, although a recent experimental study (Tan et al., 2020) in the North China Plain could not observe this effect. With many existing and developing megacities being located in subtropical regions with high emissions of reactive biogenic VOCs, control of which is very difficult, and with continuing reductions in NO_x emissions, such extreme chemical environments as that observed in Beijing can be expected to proliferate. The failure of regional and global models to accurately replicate this chemical regime has wider implications for the prediction of secondary pollutants and hence for determining policies to control air pollution episodes.

Deleted: saw no

Deleted:

Methods

The site was located at the Institute of Atmospheric Physics, between the 3rd and 4th ring road. Measurements took place between 17/05/2017 and 24/06/2017. The site is typical of central Beijing, surrounded by residential and commercial properties and is near several busy roads. It is also close to several green spaces, including a tree-lined canal to the south and the Olympic forest park to the north-east. Isoprene mixing ratios were measured by dual channel gas chromatography (DC-GC-FID). IEPOX/ISOPOOH were observed using iodide chemical ionisation mass spectrometry. The sum of MACR + MVK (m/z 71.05) was measured using proton transfer mass spectrometry. Particle samples were collected onto filter papers at either 3 hourly or 1 hourly time periods, depending on pollution levels. Filters were extracted and analysed with a high throughput method using ultra high-pressure liquid chromatography coupled to a Q-Exactive Orbitrap mass spectrometer. Nitric oxide, NO, was measured by chemiluminescence with a Thermo Scientific Model 42i NO_x analyser. Nitrogen dioxide, NO_2, was measured using a Teledyne Model T500U Cavity Attenuated Phase Shift (CAPS) spectrometer. Ozone, O_3, was measured using a Thermo Scientific Model 49i UV photometer.

DC-GC-FID

Observations of VOCs were made using a dual-channel GC with flame ionisation detectors. Air was sampled at 30 L min^{-1} at a height of 5m, through a stainless-steel manifold (½" internal diameter). 500 mL subsamples were taken, dried using a glass condensation finger held at -40°C and then pre-concentrated using a Markes Unity2 pre-concentrator on a multi-bed Ozone Precursor adsorbent trap (Markes International Ltd). These samples were then transferred to the GC oven for analysis following methods described by Hopkins et al (2011).

CIMS

A time of fight chemical ionisation mass spectrometer (ToF-CIMS) (Lee et al., 2014; Priestley et al., 2018) using an iodide ionisation system was couple deployed. Experimental set up of the University of Manchester ToF-CIMS has been previously described in Zhou et al. (2019). During the campaign, gas phase backgrounds were established by regularly overflowing the inlet with dry N_2 for 5 continuous minutes every 45 minutes and were applied consecutively. The overflowing of dry N_2 will have a small effect on the sensitivity of the instrument to those compounds whose detection is water dependent. Here we find that due to the very low instrumental background for $C_5H_{10}O_3$ and $C_5H_9NO_4$, the absolute error remains small from this effect (<10 ppt in both reported measurements).

Field calibrations were regularly carried out using known concentration formic acid gas mixtures made in a custom-made gas phase manifold. A range of other species were calibrated for after the campaign, and relative calibration factors were derived using the measured formic acid sensitivity during these calibrations, as has been performed previously (Le Breton et al. 2018, Bannan et al. 2015). In addition to this, offline calibrations, prior to and after the field work project, of a wide range of organic acids, HNO_3 and Cl_2 were performed to assess possible large scale sensitivity changes over the measurement period. No significant changes were observed. Offline calibrations after the field work campaign were performed specific to the isoprene oxidation species observed here. IEPOX ($C_5H_{10}O_3$) synthesized by the University of North Carolina, Department of Environmental Sciences & Engineering, was specifically calibrated for. Aliquots of known concentrations of IEPOX ($C_5H_{10}O_3$) were thermally desorbed into a known continuous flow of nitrogen. For $C_5H_9NO_4$ there was no direct calibration source available and concentrations using

the calibration factor of $C_5H_{10}O_3$ are presented here. Absolute measurement uncertainties are estimated at 50% for the presented IEPOX+ISOPOOH and ISOPONO2 ($C_5H_9NO_4$) signals.

Formatted: Font: Not Italic

PTR-MS

A Proton Transfer Reaction-Time of Flight-Mass Spectrometer (PTR-ToF-MS 2000, Ionicon Analytik GmBH, Innsbruck) was deployed at the base of the 325m meteorological tower at the IAP field site. This instrument has been described in detail by Jordan et al. (2009). The PTR-ToF-MS was operated at a measurement frequency of 5 Hz and an E/N ratio (where E represents the electric field strength and N the buffer gas density) in the drift tube of 130 Td. To enable accurate calibration of the mass scale trichlorobenzene was introduced by diffusion into the inlet stream.

The instrument was switched between two inlet systems in an hourly cycle. For the first 20 minutes of each hour the PTR-MS sampled from a gradient switching manifold, and for the next 40 minutes the instrument subsampled a common flux inlet line running from the 102m platform on the tower to the container in which the PTR-ToF-MS was housed. Gradient measurements were made from 3, 15, 32, 64 and 102 m with air sampled down 0.25 inch O.D. PFA lines and split between a 3 L min^{-1} bypass and 300 ml min^{-1} sample drawn to a 10 L stainless steel container. During the gradient sampling period, the PTR-ToF-MS subsampled for 2 minutes from each container giving an hourly average concentration at each height. In this work, only data from the 3m gradient height is discussed.

Zero air was generated using a platinum catalyst heated to 260 °C and was sampled hourly in the gradient switching cycle. During the field campaign, the instrument was calibrated twice weekly using a 15 component 1 ppmv VOC standard (National Physical Laboratory, Teddington). The calibration gas flow was dynamically diluted into zero air to give a six-point calibration. The sensitivity for each mass was then calculated using a transmission curve. The maximum relative error for PTR-MS calibration using a relative transmission curve has been estimated to be 21% (Taipale et al., 2008). Data was analysed using PTR-MS Viewer 3.

$PM_{2.5}$ filter sampling and analysis

$PM_{2.5}$ filter samples were collected using an ECOTECH HiVol 3000 (Ecotech, Australia) high volume air sampler with a selective $PM_{2.5}$ inlet, with a flow rate of 1.33 m^3 min^{-1}. Filters were baked at 500 ºC for five hours before use. After collection, samples were wrapped in foil and then stored at -20 ºC and shipped to the laboratory. Samples were collected at a height of 8 m, on top of a building in the IAP complex. Hourly samples were taken on 11th June between 08:00 and 17:00, with one further sample taken overnight. The extraction of the organic aerosol from the filter samples was based on the method of Hamilton et al. (2008). Initially, roughly an 8^{th} of the filter was cut up into 1 cm^2 pieces. 4 ml of LC-MS grade H_2O was then added to the sample and it was left for two hours. The samples were then sonicated for 30 minutes. Using a 2 ml syringe, the water extract was then pushed through a 0.22µm filter (Millipore) into another sample vial. An additional 1 mL of water was added to the filter sample, then extracted through the filter, to give a combined aqueous extract. This extract was then reduced to dryness using a vacuum solvent evaporator (Biotage, Sweden). The dry sample was then reconstituted in 1 mL 50:50 MeOH:H_2O solution, ready for analysis.

The extracted filter samples and standards were analysed using UPLC-MS^2, using an Ultimate 3000 UPLC (Thermo Scientific, USA) coupled to a Q-exactive Orbitrap MS (Thermo Fisher Scientific, USA) with a heated electrospray ionisation (HESI). The UPLC method uses a reverse phase 5 µm, 4.6 x 100mm, Accucore column (Thermo scientifc, UK) held at 40 ºC. The mobile phase consists of LC-MS grade water and 100 % MeOH (Fisher Chemical, USA). The water was acidified using 0.1 % formic acid to improve peak resolution. The injection volume was 2 µl. The solvent gradient was held for a minute at 90:10 H_2O:MeOH, the gradient then changed linearly to 10:90 H_2O:MeOH over 9 minutes, it was then held for 2 minutes at this gradient before returning to 90:10 H_2O:MeOH over 2 minutes and then held at 90:10 for the remaining 2 minutes, with a flow rate of 300 µL min^{-1}. The mass spectrometer was operated in negative mode using full scan MS^2. The electrospray voltage was 4.00 kV, with capillary and auxiliary gas temperatures of 320 ºC. The scan range was set between 50 - 750 m/z. Organosulfates were quantified using an authentic standard of 2-MGA-OS obtained from J. Surratt using the method described in Bryant et al. (2019).

OH measurements

The OH radical measurements were made from the roof of the University of Leeds FAGE instrument container at the IAP field site. Two Fluorescence Assay by Gas Expansion (FAGE) detection cells were housed in a weather-proof enclosure at a sampling height of approximately 4 m. OH and HO_2 radicals were detected sequentially in the first cell (the HO_x cell), whilst HO_2^* and total RO_2 radical observations were made using the second FAGE cell (the RO_x cell), which was coupled with a flow reactor to facilitate RO_2 detection (Whalley et al., 2018). A Nd:YAG pumped Ti:Sapphire laser was used to generate 5 kHz pulsed tunable UV light at 308 nm and used to excite OH via the Q1(1) transition of the $\mathbf{A^2\Sigma^+, v' = 0 \leftarrow X^2\Pi_i, v'' = 0}$ band. On-resonance fluorescence was detected using a gated micro-channel plate photomultiplier and photon counting. A background signal from laser and solar scatter and detector noise was determined by scanning the laser wavelength away from the OH transition (OHWAVE-BKD). For the entire campaign the HO_x cell was equipped with an inlet pre injector (IPI) which chemically scavenged ambient OH by periodically injecting propane into the air stream just above the FAGE inlet. The removal of ambient OH by chemical reaction provided an alternative means to determine the background signal ($OH_{CHEM\text{-}BKD}$) without the need to tune the laser wavelength. By comparison with $OH_{WAVE\text{-}BKD}$, $OH_{CHEM\text{-}BKD}$ was used to identify if any OH was generated internally within the FAGE cell, acting as an interference signal. In general, good agreement between $OH_{CHEM\text{-}BKD}$ and $OH_{WAVE\text{-}BKD}$ was observed, with a ratio of 1.07 for the whole campaign (Woodward-Massey, 2018). In this paper, the OH_{CHEM} observations are used. The instrument was calibrated every few days by over-flowing the detection cell inlet with a turbulent flow of high purity humid air containing a known concentration of OH (and HO_2) radicals generated by photolysing a known concentration of H_2O vapour at 185 nm. The product of the photon flux at 185 nm and the time spent in the photolysis region was measured before and after the campaign using N_2O actinometry (Commane et al., 2010).

OH reactivity measurements

OH reactivity measurements were made using a laser flash photolysis pump-probe technique (Stone et al., 2016). Ambient air, sampled from the roof of the FAGE container, was drawn into a reaction cell at a flow rate of 15 SLM. A 1 SLM flow of high purity, humidified air which had passed by a Hg lamp,

generating ~50 ppbv of ozone, was mixed with the ambient air at the entrance to the reaction cell. The ozone present was photolysed by 266 nm laser light at a pulse repetition frequency of 1 Hz along the central axis of the reaction cell, leading to the generation of a uniform profile of OH radicals following the reaction of $O(^1D)$ with H_2O vapour. The decay in the OH radical concentration by reaction with species present in the ambient air was monitored by sampling a portion of the air into a FAGE cell positioned at the end of the reaction cell. A fraction of the 5 kHz, 308 nm radiation generated by the Ti:Sapphire laser passed through the OH reactivity FAGE cell perpendicular to the air stream, electronically exciting the OH radicals, and the subsequent laser-induced fluorescence signal was detected with a gated channel photomultiplier tube. The 1 Hz OH decay profiles were integrated for 5 minutes and fitted to a first-order rate equation to determine the observed loss rate of OH (k_{obs}). The total OH reactivity, k(OH), was calculated by subtracting the rate coefficient associated with physical losses of OH (k_{phys}) from k_{obs}. k_{phys} was determined by monitoring the decay of OH when the ambient air was replaced with a flow of 15 SLM high purity air. A small correction to account for dilution of the ambient air by the 1 SLM flow of ozone-containing synthetic air was also applied.

Box Modelling

The box modelling that feeds into Figure 3 was performed using the Dynamically Simple Model of Atmospheric Chemical Complexity (DSMACC), zero-dimensional box model (Emmerson and Evans, 2009), together with the isoprene scheme, together with the relevant inorganic chemistry, from the near explicit chemical mechanism the Master Chemical Mechanism (MCM) v3.3.1 (Jenkin et al., 1997; Jenkin et al., 2015). The complete isoprene degradation mechanism in MCM v3.3.1 consists of 1926 reactions of 602 closed shell and free radical species, which treat the chemistry initiated by reaction with OH radicals, NO_3 radicals and ozone. It contains much of the isoprene HO_X recycling chemistry identified as important in recent years under "low NO" conditions, including the peroxy radical 1,4 and 1,6 H-shift chemistry described in the LIM1 mechanism (Peeters et al., 2009; 2014), as summarized in Wennberg et al. (2018). Model photolysis rates were calculated using the Tropospheric Ultraviolet and Visible Radiation Model (TUV v5.2) (Madronich, 1993).

The box model was initialised with a range of different concentrations of isoprene (1.7 ppb, 3.4 ppb, 5.0 ppb, 6.7 ppb), and OH (0.25, 0.5, 1.0, 3.0, 10, 20 × 10^6 cm^{-3}). [CH_4] was fixed at 1.85 ppmv and [CO] at 110 ppbv, T = 298 K, and [H_2O] = 2.55 × 10^{17} cm^{-3}. Entrainment loss rates for all model species were set to 1 × 10^{-5} cm^{-3} s^{-1}. For the box model, a column average value for deposition velocity, V_d, was calculated according to the functionalities of each species (Table S2). These terms prevent the build-up of secondary products. The values are based on reported deposition rates in Nguyen et al. (2015). A boundary layer height (*BLH*) of 1.5 km was assumed. Loss rates (L_d) for each species to dry deposition are then $L_d = V_d/BLH$. Photolysis rates were fixed to mean rates for the day time period 09:00-17:00 calculated for July 1. The model was then run to steady state for a range of fixed NO mixing ratios from 0 – 16,000 pptv.

GEOS-Chem Modeling

GEOS-Chem version 11-01 (http://wiki.seas.harvard.edu/geos-chem/index.php/GEOS-Chem_v11-01) with the inclusion of the aromatic component of RACM2 (regional atmospheric chemistry mechanism 2) was run nested at 0.25 x 0.3125 degree resolution, with 4 x 5 degree boundary conditions using GEOS-FP meteorology. The NO emissions were added via the default MIX emission inventory, which required a 0.9x multiplier on the total daily emissions to match observations from the APHH summer campaign. The diurnal scale factor was considerably steeper than the default GEOS-Chem NO diurnal, with a day-time scale factor on the order of 1.7x and a 0.25x night-time multiplier. Isoprene emissions calculated by the MEGAN biogenic emissions extension were scaled by 2.5x in the Beijing metropolitan region (Jing-Jin-Ji).

Data availability

Data are available at http://catalogue.ceda. ac.uk/uuid/7ed9d8a288814b8b85433b0d3fec0300 (last access: 13 Feb 2020). Specific data are available from the authors on request (jacqui.hamilton@york.ac.uk).

Author Contributions

JRH, RED, JFH, WJFA, CNH, BL and XW provided the VOC measurements. FAS, WSD and JDL provided the NO_x and O_3 measurements. TJB, AM, SDW, AB, CJP and HC collected and analysed the CIMS data. TQ and JDS provided the organo-sulfate standards. DB, WD and JFH provided the organo-sulfate aerosol measurements. LKW, DEH, EJS, RW-M and CY provided the OH and HO_2 data. MN, PME and ARR provided the MCM box modelling. PDI and MJE provided the GEOS-Chem model run. ACL is the PI of the AIRPRO-Beijing project. MJN, JFH and ARR conceived and wrote the manuscript with input and discussion from all co-authors.

Competing Interests

The authors declare that they have no conflict of interest.

Acknowledgements

This project was funded by the Natural Environment Research Council, the Newton Fund and Medical Research Council in the UK, and the National Natural Science Foundation of China (NE/N007190/1, NE/N006917/1). We acknowledge the support from Pingqing Fu, Zifa Wang, Jie Li and Yele Sun from IAP for hosting the APHH-Beijing campaign at IAP. We thank Zongbo Shi, Roy Harrison, Tuan Vu and Bill Bloss from the University of Birmingham, Siyao Yue, Liangfang Wei, Hong Ren, Qiaorong Xie, Wanyu Zhao, Linjie Li, Ping Li, Shengjie Hou, Qingqing Wang from IAP, Kebin He and Xiaoting Cheng from Tsinghua University, and James Allan from the University of Manchester for providing logistic and scientific support for the field campaigns. Peter Ivatt acknowledges funding from NCAS through one of its Air Quality and Human Health studentships. Daniel Bryant, William Dixon, William Drysdale, Freya Squires and Eloise Slater acknowledge the NERC SPHERES Doctoral Training Programme (DTP) for studentships.

References

Air Quality Expert Group: Ozone in the United Kingdom, Department for the Environment, Food and Rural Affairs, http://www.defra.gov.uk/environment/airquality/aqeg, 2009.

Bannan, T. J., Booth, A. M., Bacak, A., Muller, J. B. A., Leather, K. E., Le Breton, M., Jones, B., Young, D., Coe, H., Allan, J., Visser, S., Slowik, J. G., Furger, M., Prevot, A. S. H., Lee, J. Dunmore, R. E., Hopkins, J. R., Hamilton, J. F., Lewis, A. C., Whalley, L. K., Sharp, T., Stone, D., Heard, D. E., Fleming, Z. L., Leigh, R., Shallcross, D. E., and Percival, C. J.: The first U.K. measurements of nitryl chloride using a chemical ionisation mass spectrometer in London, ClearfLo Summer, 2012, and an investigation of the role of Cl atom oxidation. Journal of Geophysical Research, 120, 5638-5657, 2015.

Bannan, T. J., Le Breton, M., Priestley, M., Worrall, S. D., Bacak, A., Marsden, N. A., Mehra, A., Hammes, J., Hallquist, M., Alfarra, M. R., Krieger, U. K., Reid, J. P., Jayne, J., Robinson, W., McFiggans, G., Coe, H., Percival, C. J., and Topping, D.: A method for extracting calibrated volatility information from the FIGAERO-HR-ToF-CIMS and its experimental application, Atmos. Meas. Tech., 12, 1429–1439, https://doi.org/10.5194/amt-12-1429-2019, 2019.

Bianchi F., Kurtén, T., Riva, M., Mohr, C., Rissanen, M. P., Roldin, P., Berndt, T., Crounse, J. D., Wennberg, P. O., Mentel, T. F., Wildt, J., Junninen, H., Jokinen, T., Kulmala, M., Worsnop, D. R., Thornton, J. A., Donahue, N. Kjaergaard, H. G., and Ehn, M.: Highly Oxygenated Organic Molecules (HOM) from Gas-Phase Autoxidation Involving Peroxy Radicals: A Key Contributor to Atmospheric Aerosol, Chem. Rev., 119, 3472-3509, 2019.

Brean, J., Harrison, R. M., Shi, Z., Beddows, D. C. S., Acton, W. J. F., Hewitt, C. N., Squires, F. A., and Lee, J.: Observations of highly oxidized molecules and particle nucleation in the atmosphere of Beijing, Atmos. Chem. Phys., 19, 14933–14947, https://doi.org/10.5194/acp-19-14933-2019, 2019.

Bryant, D. J., Dixon, W. J., Hopkins, J. R., Dunmore, R. E., Pereira, K. L., Shaw, M., Squires, F. A., Bannan, T. J., Mehra, A., Worrall, S. D., Bacak, A., Coe, H., Percival, C. J., Whalley, L. K., Heard, D. E., Slater, E. J., Ouyang, B., Cui, T., Surratt, J. D., Liu, D., Shi, Z., Harrison, R., Sun, Y., Xu, W., Lewis, A. C., Lee, J. D., Rickard, A. R., and Hamilton, J. F.: Strong anthropogenic control of secondary organic aerosol formation from isoprene in Beijing, Atmos. Chem. Phys. Discuss., https://doi.org/10.5194/acp-2019-929, in review, 2019.

Chan, A. W. H., Chan, M. N., Surratt, J. D., Chhabra, P. S., Loza, C. L., Crounse, J. D., Yee, L. D., Flagan, R. C., Wennberg, P. O., and Seinfeld, J. H.: Role of aldehyde chemistry and NO_x concentrations in secondary organic aerosol formation, Atmos. Chem. Phys., 10, 7169–7188, https://doi.org/10.5194/acp-10-7169-2010, 2010.

Cheng, J., Su, J., Cui, T., Li, X., Dong, X., Sun, F., Yang, Y., Tong, D., Zheng, Y., Li, Y., Li, J., Zhang, Q., and He, K.: Dominant role of emission reduction in PM2.5 air quality improvement in Beijing during 2013–2017: a model-based de- composition analysis, Atmos. Chem. Phys., 19, 6125–6146, 2019.

Commane, R., Floquet, C. F. A., Ingham, T., Stone, D., Evans, M. J., and Heard, D. E.: Observations of OH and HO_2 radicals over West Africa, Atmos. Chem. Phys., 10, 8783–8801, https://doi.org/10.5194/acp-10-8783-2010, 2010.

Crounse, J. D., Nielsen, L. B., Jørgensen, S., Kjaergaard, H. G., and Wennberg, P.: Autooxidation of Organic Compounds in the Atmosphere, J. Phys. Chem. Lett., 4, 3513-3520, 2013.

Emmerson, K. M., and Evans, M. J.: Comparison of tropospheric gas-phase chemistry schemes for use within global models, Atmos. Chem. Phys., 9, 1831-1845, https://doi.org/10.5194/acp-9-1831-2009, 2009.

Hamilton, J. F., Lewis, A.C., Carey, T. J., and Wenger, J. C.: Characterization of Polar Compounds and Oligomers in Secondary Organic Aerosol Using Liquid Chromatography Coupled to Mass Spectrometry, Anal. Chem., 80, 474-480, 2008.

Hopkins, J. R., Jones, C. E., and Lewis, A. C.: A dual channel gas chromatograph for atmospheric analysis of volatile organic compounds including oxygenated and monoterpene compounds, J. Environ. Monit., 13, 2268-2276, 2011.

Jenkin, M. E., Saunders, S. M., and Pilling, M. J.: The tropospheric degradation of volatile organic compounds: a protocol for mechanism development, Atmos. Environ., 31, 81–104, 1997.

Jenkin, M. E., Young, J. C., and Rickard, A. R. R.: The MCM v3.3.1 degradation scheme for isoprene, Atmos. Chem. Phys., 15, 11433-11459, 2015.Hofzumahaus, A., Rohrer, F., Lu, K., et al.: Amplified Trace Gas Removal in the Troposphere, Science, 324, 1702-1704, 2009.

Jimenez, J. L., Canagaratna, M. R., Donahue, Prevot, A. S. H., Zhang, Q., Kroll, J. H. DeCarlo, P. F., Allan, J. D., Coe, H., Ng, N. L., Aiken, A. C., Docherty, K. S., Ulbrich, I. M., Grieshop, A. P., Robinson, A. L., Duplissy, J., Smith, J. D., Wilson, K. R., Lanz, V. A., Hueglin, C., Sun, Y. L., Tian, J., Laaksonen, A., Raatikainen, T., Rautiainen, J., Vaattovaara, P., Ehn, M., Kulmala, M., Tomlinson, J. M., Collins, D. R., Cubison, M. J., Dunlea, E. J., Huffman, J. A., Onasch, T. B., Alfarra, M. R., Williams, P. I., Bower, K., Kondo, Y., Schneider, J., Drewnick, F., Borrmann, S., Weimer, S., Demerjian, K., Salcedo, D., Cottrell, L., Griffin, R., Takami, A., Miyoshi, T., Hatakeyama, S., Shimono, A., Sun, J. Y., Zhang, Y. M., Dzepina, K., Kimmel, J. R., Sueper, D., Jayne, J. T., Herndon, S. C., Trimborn, A. M., Williams, L. R., Wood, E. C.. Middlebrook, A. M., Kolb, C. E., Baltensperger, U., and Worsnop, D. R.: Evolution of Organic Aerosols in the Atmosphere, Science, 326, 1525-1529, 2009.

Jordan, A., Haidacher, S., Hanel, G., Hartungen, E., Märk, L., Seehauser, H., Schottkowsky, R., Sulzer, P., and Märk T.D.: A high resolution and high sensitivity proton-transfer-reaction time-of-flight mass spectrometer (PTR-TOF-MS), Int. J. Mass Spectrom., 286, 122-128, 2009.

Kroll, J. H., Ng, N. L., Murphy, S. M., Flagan, R. C., and Seinfeld, J. H.: Secondary organic aerosol formation from isoprene photooxidation, Environ. Sci. Technol., 40, 1869–1877, 2006.

Krotkov, N. A., McLinden, C. A., Li, C., Lamsal, L. N., Celarier, E. A., Marchenko, S. V., Swartz, W. H., Bucsela, E. J., Joiner, J., Duncan, B. N., Boersma, K. F., Veefkind, J. P., Levelt, P. F., Fioletov, V. E., Dickerson, R. R., He, H., Lu, Z., and Streets, D. G.: Aura OMI observations of regional SO_2 and NO_2 pollution changes from 2005 to 2015, Atmos. Chem. Phys., 16, 4605–4629, 2016.

Le Breton, M., Wang, Y., Hallquist, Å. M., Pathak, R. K., Zheng, J., Yang, Y., Shang, D., Glasius, M., Bannan, T. J., Liu, Q., Chan, C. K., Percival, C. J., Zhu, W., Lou, S., Topping, D., Wang, Y., Yu, J., Lu, K., Guo, S., Hu, M., and Hallquist, M.: Online gas- and particle-phase measurements of organosulfates, organosulfonates and nitrooxy organosulfates in Beijing utilizing a FIGAERO ToF-CIMS, Atmos. Chem. Phys., 18, 10355-10371, https://doi.org/10.5194/acp-18-10355-2018, 2018.

Lee, B. H., Lopez-Hilfiker, F. D., Mohr, C., Kurtén, T., Worsnop, D. R., and Thornton, J. A.: An iodide-adduct high-resolution time-of-flight chemical-ionization mass spectrometer: Application to atmospheric inorganic and organic compounds, Environ. Sci. Technol., 48, 6309-6317, 2014.

Li, K., Jacob, D. J., Liao, H., Shen, L., Zhang, Q., and Bates, K. H.: Anthropogenic drivers of 2013-2017 trends in summer surface ozone in China, Proc. Natl. Acad. Sci., 116, 422-427, 2019.

Li, Q., Su, G., Li, C., Liu, P., Zhao, X., Zhang, C., Sun, X., Mu, Y., Wu, M., Wang, Q., and Sun, B.: An investigation into the role of VOCs in SOA and ozone production in Beijing, China, Sci. Total Environ., 720, doi: 10.1016/j.scitotenv.2020.137536, 2020.

Lin, Y-H., Zhang, Z., Docherty, K. S., Zhang, H., Budisulistiorini, S. H., Rubitschin, C. L., Shaw, S. L., Knipping, E. M., Edgerton, E. S., Kleindienst, T. E., Gold, A., Surratt, J. D.: Isoprene Epoxydiols as Precursors to Secondary Organic Aerosol Formation: Acid-Catalyzed Reactive Uptake Studies with Authentic Compounds, Environ. Sci. Technol., 46, 250-258, 2012.

Lin, Y. -H., Zhang, H., Pye, H. O. T., Zhang, Z., Marth, W. J., Park, S., Arashiro, M., Cui, T., Budisulistiorini, S. H., Sexton, K. G., Vizuete, W., Xie, Y., Luecken, D. J., Piletic, I. R., Edney, E. O., Bartolotti, L.J., Gold, A., and Surratt, J. D.: Epoxide as a precursor to secondary organic aerosol formation from isoprene photooxidation in the presence of nitrogen oxides, Proc. Natl. Acad. Sci., 110, 6718-6723, https://doi.org/10.1073/pnas.1221150110, 2013

Liu, F., Zhang, Q., van der A, R. J., Zheng, B., Tong, D., Yan, L., Zheng, Y., and He, K.: Recent reduction in NOx emissions over China: synthesis of satellite observations and emission inventories, Environ. Res. Lett., 11, 114002, 2016.

Liu, H., Zhang, M., Han, X., Li, J., Chen, L.: Episode analysis of regional contributions to tropospheric ozone in Beijing using a regional air quality model, Atmos. Environ., 199, 299-312, 2019.

Lopez-Hilfiker, F. D., Mohr, C., Ehn, M., Rubach, F., Kleist, E., Wildt, J., Mentel, Th. F., Lutz, A., Hallquist, M., Worsnop, D., and Thornton, J. A.: A novel method for online analysis of gas and particle composition: description and evaluation of a Filter Inlet for Gases and AEROsols (FIGAERO), Atmos. Meas. Tech., 7, 983–1001, https://doi.org/10.5194/amt-7-983-2014, 2014.

Madronich, S.: The Atmosphere and UV-B Radiation at Ground Level. In: Young, A. R., Moan, J., Björn, L. O., Nultsch, W., editors. Environmental UV Photobiology. Boston, MA, Springer US, pp. 1-39., 1993.

Miyazaki, K., Eskes, H., Sudo, K., Boersma, K. F., Bowman, K., and Kanaya, Y.: Decadal changes in global surface NO_xemissions from multi-constituent satellite data assimilation, Atmos. Chem. Phys., 17, 807–837, 2017.

Nguyen, T. B., Crounse, J. D., Teng, A. P., Clair, J. M. S., Paulot, F., Wolfe, G. M., and Wennberg, P. O.: Rapid deposition of oxidized biogenic compounds to a temperate forest, Proc. Natl. Acad. Sci., 112, E392-E401, 2015.

Nguyen, T. B., Bates, K. H., Crounse, J. D., Schwantes, R. H., Zhang, X., Kjaergaard, H. G., Surratt, J. D., Lin, P., Laskin, A., Seinfeld, J. H., and Wennberg, P. O.: Mechanism of the hydroxyl radical oxidation of methacryloyl peroxynitrate (MPAN) and its pathway toward secondary organic aerosol formation in the atmosphere, Phys. Chem. Chem. Phys., 17, 17914–17926, https://doi.org/10.1039/C5CP02001H, 2015.

Orlando, J. J., and Tyndall, G. S.: Laboratory studies of organic peroxy radical chemistry: an overview with emphasis on recent issues of atmospheric significance, Chem. Soc. Rev., 41, 6294-6317, 2012.

Paulot, F., Crounse, J. D., Kjaergaard, H. G., Kürten, A., St. Clair, J. M., Seinfeld, J. H., and Wennberg, P. O.: Unexpected epoxide formation in the gas-phase photooxidation of isoprene, Science, 325, 730-733, 2009.

Peeters, J., Nguyen, T. L., and Vereecken, L.: HOx radical regeneration in the oxidation of isoprene, Phys. Chem. Chem. Phys., 11, 5935-5939, 2009.

Peeters, J., Müller, J. -F., Stavrakou, T., and Nguyen, V. S.: Hydroxyl Radical Recycling in Isoprene Oxidation Driven by Hydrogen Bonding and Hydrogen Tunneling: The Upgraded LIM1 Mechanism, J. Phys. Chem. A., 118, 8625-8643, 2014.

Praske, E., Otkjaer, R. V., Crounse, J. D., Hethcox, J. C., Stoltz, B. M., Kjaergaard, H. G., and Wennberg, P. O.: Atmospheric autoxidation is increasingly important in urban and suburban North America, Proc. Natl. Acad. Sci., 115, 64-69, 2018.

Priestley, M., Le Breton, M., Bannan, T. J., Leather, K. E., Bacak, A., Reyes-Villegas, E., de Vocht, F., Shallcross, B. M. A., Brazier, T., Khan, M. A., Allan, J., Shallcross, D. E., Coe, H., Percival, C. J.: Observations of isocyanate, amide, nitrate and nitro compounds from an anthropogenic biomass burning event using a ToF-CIMS, J Geophys. Res. Atmos., 123, 7687-7704, 2018.

Reeves, C. E., et al.: Observations of speciated isoprene nitrates in Beijing: implications for isoprene chemistry, Atmos. Chem. Phys. Discuss., https://doi.org/10.5194/acp-2019-964, in review, 2020.

Ren, X., Harder, H., Martinez, M., Lesher, R. L., Oliger, A., Simpas, J. B., Brune, W. H., Schwab, J. J., Demerjian, K. L., He, Y., Zhou, X., and Gao, H.: OH and HO_2 chemistry in the urban atmosphere of New York City, Atmos. Environ., 37, 3639–3651, 2003.

Rivera-Rios, J. C., Nguyen, T. B., Crounse, J. D., Jud, W., St. Clair, J. M., Mikoviny, T., Gilman, J. B., Lerner, B. M., Kaiser, J. B., de Gouw, J., Wisthaler, A., Hansel, A., Wennberg, P. O., Seinfeld, J. H., and Keutsch, F. N.: Conversion of hydroperoxides to carbonyls in field and laboratory instrumentation: Observational bias in diagnosing pristine versus anthropogenically controlled atmospheric chemistry, Geophys. Res. Lett., 41, 8645–8651, doi:10.1002/ 2014GL061919, 2014.

Sanchez, D., Jeong, D., Seco, R., Wrangham, I., Park, J. H., Brune, W. H., Koss, A., Gilman, J., de Gouw, J., Misztal, P., Goldstein, A., Baumann, K., Wennberg, P. O., Keutsch, F. N., Guenther, A., and Kim. S.: Intercomparison of OH and OH reactivity measurements in a high isoprene and low NO environment during the Southern Oxidant and Aerosol Study (SOAS), Atmos. Environ., 174, 227-236, 2018.

Schwantes, R. H., Charan, S. M., Bates, K. H., Huang, Y., Nguyen, T. B., Mai, H., Kong, W., Flagan, R. C., and Seinfeld, J. H.: Low-volatility compounds contribute significantly to isoprene secondary organic aerosol (SOA) under high-NO_x conditions, Atmos. Chem. Phys., 19, 7255–7278, https://doi.org/10.5194/acp-19-7255-2019, 2019.

Shi, Z., Vu, T., Kotthaus, S., Harrison, R. M., Grimmond, S., Yue, S., Zhu, T., Lee, J., Han, Y., Demuzere, M., Dunmore, R. E., Ren, L., Liu, D., Wang, Y., Wild, O., Allan, J., Acton, W. J., Barlow, J., Barratt, B., Beddows, D., Bloss, W. J., Calzolai, G., Carruthers, D., Carslaw, D. C., Chan, Q., Chatzidiakou, L., Chen, Y., Crilley, L., Coe, H., Dai, T., Doherty, R., Duan, F., Fu, P., Ge, B., Ge, M., Guan, D., Hamilton, J. F., He, K., Heal, M., Heard, D., Hewitt, C. N., Hollaway, M., Hu, M., Ji, D., Jiang, X., Jones, R., Kalberer, M., Kelly, F. J., Kramer, L., Langford, B., Lin, C., Lewis, A. C., Li, J., Li, W., Liu, H., Liu, J., Loh, M., Lu, K., Lucarelli, F., Mann, G., McFiggans, G., Miller, M. R., Mills, G., Monk, P., Nemitz, E., O'Connor, F., Ouyang, B., Palmer, P. I., Percival, C., Popoola, O., Reeves, C., Rickard, A. R., Shao, L., Shi, G., Spracklen, D., Stevenson, D., Sun, Y., Sun, Z., Tao, S., Tong, S., Wang, Q., Wang, W., Wang, X., Wang, X., Wang, Z., Wei, L., Whalley, L., Wu, X., Wu, Z., Xie, P., Yang, F., Zhang, Q., Zhang, Y., Zhang, Y., and Zheng, M.: Introduction to the special issue “In-depth study of air pollution sources and processes within Beijing and its surrounding region (APHH-Beijing)”, Atmos. Chem. Phys., 19, 7519–7546, https://doi.org/10.5194/acp-19-7519-2019, 2019.

Sindelarova, K., Granier, C., Bouarar, I., Guenther, A., Tilmes, S., Stavrakou, T., Müller, J.-F., Kuhn, U., Stefani, P., and Knorr, W.: Global data set of biogenic VOC emissions calculated by the MEGAN model over the last 30 years, Atmos. Chem. Phys., 14, 9317-9341, https://doi.org/10.5194/acp-14-9317-2014, 2014.

Stone, D., Whalley, L. K., Ingham, T., Edwards, P. M., Cryer, D. R., Brumby, C. A., Seakins, P. W., and Heard, D. E.: Measurement of OH reactivity by laser flash photolysis coupled with laser-induced fluorescence spectroscopy, Atmos. Meas. Tech., 9, 2827–2844, https://doi.org/10.5194/amt-9-2827-2016, 2016.

Surratt, J. D., Murphy, S. M., Kroll, J. H., Ng, N. L., Hildebrandt, L., Sorooshian, A., Szmigielski, R., Vermeylen, R., Maenhaut, W., Claeys, M., Flagan, R. C., and Seinfeld, J. H.: Chemical composition of secondary organic aerosol formed from the photooxidation of isoprene, J. Phys. Chem. A., 110, 9665–9690, 2006.

Surratt, J. D., Chan, A. W. H., Eddingsaas, N. C., Chan, M. N., Loza, C. L., Kwan, A. J., Hersey, S. P., Flagan, R. C., Wennberg, P. O., and Seinfeld, J. H.: Reactive intermediates revealed in secondary organic aerosol formation from isoprene, Proc. Natl. Acad. Sci., 107, 6640-6645, 2010.

Tan, Z., Lu, K., Hofzumahaus, A., Fuchs, H., Bohn, B., Holland, F., Liu, Y., Rohrer, F., Shao, M., Sun, K., Wu, Y., Zeng, L., Zhang, Y., Zou, Q., Kiendler-Scharr, A., Wahner, A., and Zhang, Y.: Experimental budgets of OH, HO_2, and RO_2 radicals and implications for ozone formation in the Pearl River Delta in China 2014, Atmos. Chem. Phys., 19, 7129-7150, 2019.

Tang, G., Li, X., Wang, Y. Xin, J., and Ren. X.: Surface ozone trend details and interpretations in Beijing, 2001-2006, Atmos. Chem. Phys., 9, 8813-8823, 2009.

Wang, T., Xue, L., Brimblecombe, P., Lam, Y. F., Li, L., and Zhang, L.: Ozone pollution in China: A review of concentrations, meteorological influences, chemical precursors, and effects, Sci. Total. Environ., 575, 1582-1596, 2017.

Wang, Z., Li, Y., Chen, T., Zhang, D., Sun, F., Wei, Q., Dong, X., Sun, R., Huan, N., and Pan, L.: Ground-level ozone in urban Beijing over a 1-year period: Temporal variations and relationship to atmospheric oxidation, Atmos. Res., 164-165, 110-117, 2015.

Wennberg, P. O., Bates, K. H., Crounse, J. D., Dodson, L. G., McVay, R. C., Mertens, L. A., Nguyen, T. B., Praske, E., Schwantes, R. H., Smarte, M. D., St. Clair, J. M., Teng, A. P., Zhang, X., and Seinfeld J. H.: Gas-phase reactions of isoprene and its major oxidation products, Chem. Rev., 118, 3337-3390, 2018.

Whalley, L. K., Edwards, P. M., Furneaux, K. L., Goddard, A., Ingham, T., Evans, M. J., Stone, D., Hopkins, J. R., Jones, C. E., Karunaharan, A., Lee, J. D., Lewis, A. C., Monks, P. S., Moller, S. J., and Heard, D. E.: Quantifying the magnitude of a missing hydroxyl radical source in a tropical rainforest, Atmos. Chem. Phys., 11, 7223-7233, https://doi.org/10.5194/acp-11-7223-2011, 2011.

Whalley, L. K., Stone, D., Bandy, B., Dunmore, R., Hamilton, J. F., Hopkins, J., Lee, J. D., Lewis, A. C., and Heard, D. E.: Atmospheric OH reactivity in central London: observations, model predictions and estimates of in situ ozone production, Atmos. Chem. Phys., 16, 2109-2122, https://doi.org/10.5194/acp-16-2109-2016, 2016.

Whalley, L. K., Stone, D., Dunmore, R., Hamilton, J., Hopkins, J. R., Lee, J. D., Lewis, A. C., Williams, P., Kleffmann, J., Laufs, S., Woodward-Massey, R., and Heard, D. E.: Understanding in situ ozone production in the summertime through radical observations and modelling studies during the Clean air for London project (ClearfLo), Atmos. Chem. Phys., 18, 2547-2571, https://doi.org/10.5194/acp-18-2547-2018, 2018.

Whalley, L. K., Slater, E. J., Woodward-Massey, R., Ye, C., Lee, J. D., Squires, F., Hopkins, J. R., Dunmore, R. E., Shaw, M., Hamilton, J. F., Lewis, A. C., Mehra, A., Worrall, S. D., Bacak, A., Bannan, T. J., Coe, H., Ouyang, B., Jones, R. L., Crilley, L. R., Kramer, L. J., Bloss, W. J., Vu, T., Kotthaus, S., Grimmond, S., Sun, Y., Xu, W., Yue, S., Ren, L., Acton, W. J. F., Hewitt, C. N., Wang, X., Fu, P., and Heard, D. E.: Evaluating the sensitivity of radical chemistry and ozone formation to ambient VOCs and NO_x in Beijing, Atmos. Chem. Phys. Discuss., https://doi.org/10.5194/acp-2020-785, in review, 2020.

Woodward-Massey, R.: Observations of radicals in the atmosphere: measurement validation and model comparisons, PhD Thesis, University of Leeds, 2018.

Xiong, F., McAvey, K. M., Pratt, K. A., Groff, C. J., Hostetler, M. A., Lipton, M. A., Starn, T. K., Seeley, J. V., Bertman, S. B., Teng, A. P., Crounse, J. D., Nguyen, T. B., Wennberg, P. O., Misztal, P. K., Goldstein, A. H., Guenther, A. B., Koss, A. R., Olson, K. F., de Gouw, J. A., Baumann, K., Edgerton, E. S., Feiner, P. A., Zhang, L., Miller, D. O., Brune, W. H., and Shepson, P. B.: Observation of isoprene hydroxynitrates in the southeastern United States and implications for the fate of NO_x, Atmos. Chem. Phys., 15, 11257–11272, https://doi.org/10.5194/acp-15-11257-2015, 2015.

Zhang, Q., Zheng, Y. X., Tong, D., Shao, M., Wang, S. X., Zhang, Y. H., Xu, X. D., Wang, J. N., He, H., Liu, W. Q., Ding, Y. H., Lei, Y., Li, J. H., Wang, Z. F., Zhang, X. Y., Wang, Y. S., Cheng, J., Liu, Y., Shi, Q. R., Yan, L., Geng, G. N., Hong, C. P., Li, M., Liu, F., Zheng, B., Cao, J. J., Ding, A. J., Gao, J., Fu, Q. Y., Huo, J. T., Liu, B. X., Liu, Z. R., Yang, F. M., He, K. B., and Hao, J. M.: Drivers of improved PM2.5 air quality in China from 2013 to 2017, Proc. Natl. Acad. Sci., 116, 24463–24469, 2019.

Zhou, W., Zhao, J., Ouyang, B., Mehra, A., Xu, W., Wang, Y., Bannan, T. J., Worrall, S. D., Priestley, M., Bacak, A., Chen, Q., Xie, C., Wang, Q., Wang, J., Du, W., Zhang, Y., Ge, X., Ye, P., Lee, J. D., Fu, P., Wang, Z., Worsnop, D., Jones, R., Percival, C. J., Coe, H., and Sun, Y.: Production of N2O5 and ClNO2 in summer in urban Beijing, China, Atmos. Chem. Phys., 18, 11581-11597, https://doi.org/10.5194/acp-18-11581-2018, 2018.

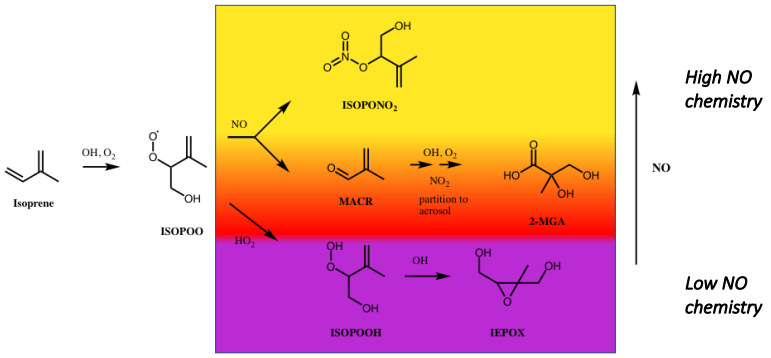

Figure 1: Formation pathways of isoprene oxidation products used as tracers of high / low-NO chemistry in this work. Following reaction of the primary VOC, isoprene, with OH, a peroxy radical intermediate (ISOPOO) is formed. At low NO concentrations, ISOPOO reacts with HO_2 (or other RO_2), to yield hydroperoxide (ISOPOOH) isomers ((4,3)-ISOPOOH isomer is shown), which can be rapidly oxidized to isoprene epoxydiol (IEPOX) isomers. At high NO concentrations, ISOPOO reacts with NO, a minor product of which is an isoprene nitrate (ISOPONO2). One of the major products of ISOPOO reaction with NO is methacrolein (MACR), the subsequent oxidation of which, in the presence of NO_2, can lead to 2-methylglyceric acid (2-MGA) and its corresponding oligomers and organosulfates in the aerosol phase. Measurements of these products in the gas or aerosol phase can be used as tracers for the chemical environment in which they were formed.

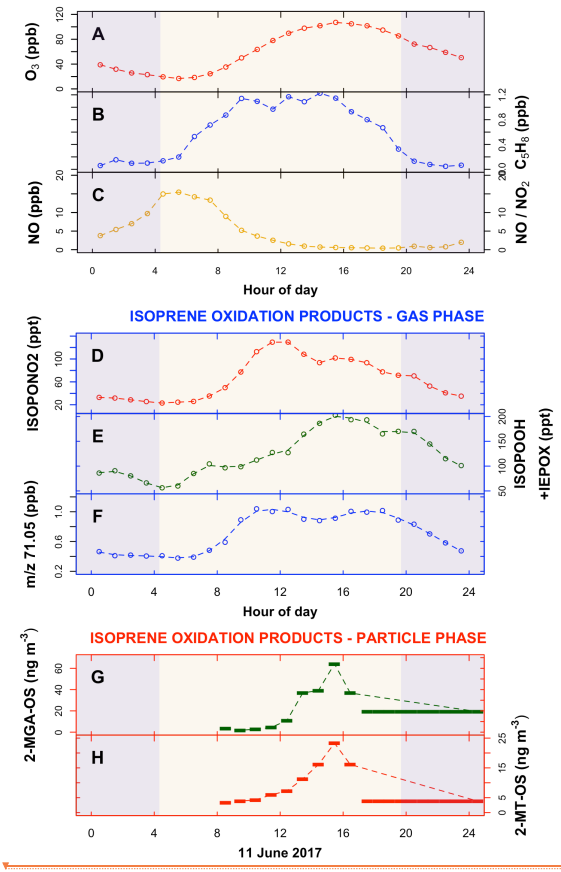

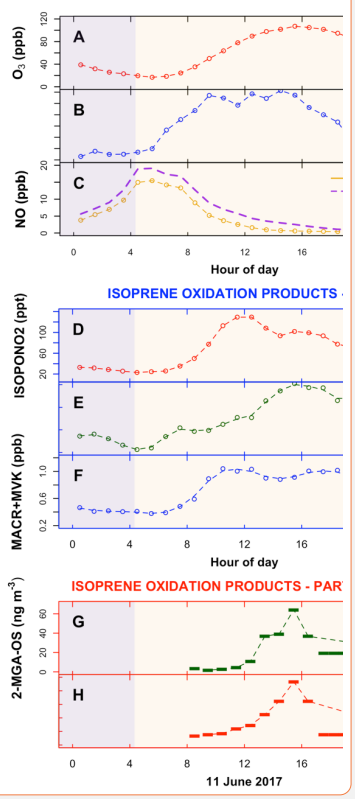

Figure 2: Mean diurnal variation of measured organic and inorganic species in the gas phase and aerosol during the Beijing summer observations (data is filtered to only include 'typical' chemistry days – see text for details; the standard deviation of the mean is shown in Figure S3). Blue shaded areas are night-time. a. ozone (O_3); (b) isoprene (C_5H_8); (c) nitric oxide (NO) and the ratio NO / NO_2; (d) the gas phase isoprene 'high NO' oxidation product, isoprene nitrate (ISOPONO2); (e) the isoprene 'low NO' oxidation products ISOPOOH + IEPOX; (f) m/z 71.05, assumed to be predominantly the gas phase isoprene 'high NO' oxidation products methacrolein (MACR) (precursor to 2-MGA) + methyl vinyl ketone (MVK), signal calibrated with MACR/MVK – see text for further details. (g&h) SOA components: 2-methyltetrol-organosulfate (2-MT-OS) and 2-methylglyceric acid-organosulfate (2-MGA-OS), both measured on the 11/12th June 2017, the last filter sample was taken from 17:30 11 June - 08:30 12 June.

Deleted: ; the standard deviation of the mean is shown in Figure S3…. Blue shaded areas are night-time. a. Mean diurnal cycle of the inorganic species NO and o…zone (O_3); (b) and of the product precursor …i…oprene (C_5H_8)…. Shaded areas are at night; area between the dotted lines indicates where > 25% of the isoprene chemistry is driven by low NO pathways (Fig. 3). Mean diurnal cycles of: …b… ... [1]

Formatted: Subscript

Deleted: c…) the isoprene 'low NO' oxidation products ISOPOOH + IEPOX; (d…) m/z 71.05, assumed to be predominantly the gas phase isoprene 'high NO' oxidation products methacrolein (MACR) (precursor to 2-MGA) + methyl vinyl ketone (MVK), signal calibrated with MACR/MVK – see text for further details. (e…&hf [2]

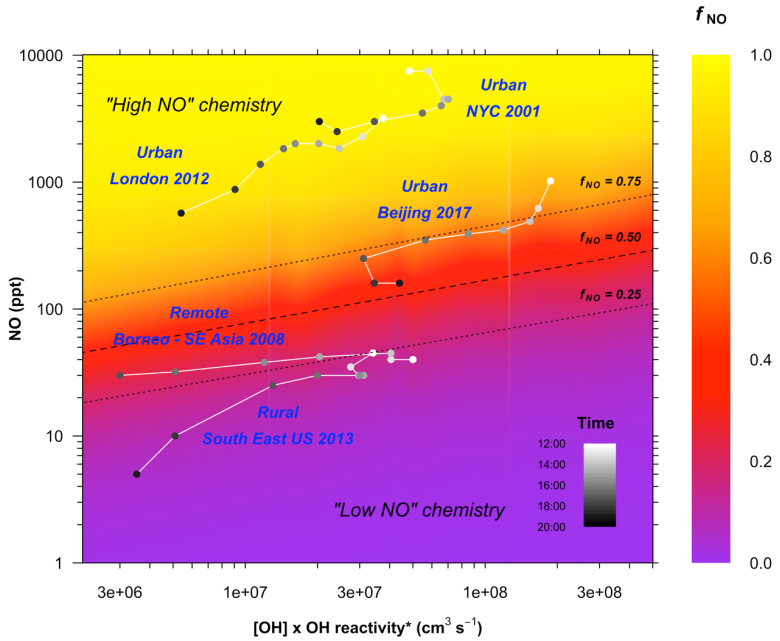

Figure 3: Variation of the fraction of ISOPOO reacting with NO as a function of NO concentration and the reactivity of the system. The plot is derived from a series of zero-dimensional box model runs performed as a function of fixed concentrations of [NO], [OH], and [isoprene]. Photolysis is fixed to an average of 09:00-17:00 conditions. OH reactivity* is total OH reactivity of the chemical system minus the contribution from OH + NOx (Equation E1), since these reactions do not produce RO2.

$$\text{OH reactivity*} = \sum \boldsymbol{k_{OH+VOC}}\,[\text{VOC}] \quad \text{(E1)}$$

The dashed line shows the fraction of ISOPOO reacting with NO $f_{NO} = 0.50$, dotted lines show $f_{NO} = 0.25$ and 0.75. Points are average diurnal hourly measurements of NO, OH, and OH reactivity* for the period 12:00 – 20:00 pm from a range of different environments: The rural sites, Borneo (Whalley et al., 2011) (only shown for 12:00-18:00) and the Southeast US (Sanchez et al., 2018), and the urban sites London (Whalley et al., 2016), New York City (Ren et al., 2003), and Beijing (this work). See the SI for full details.

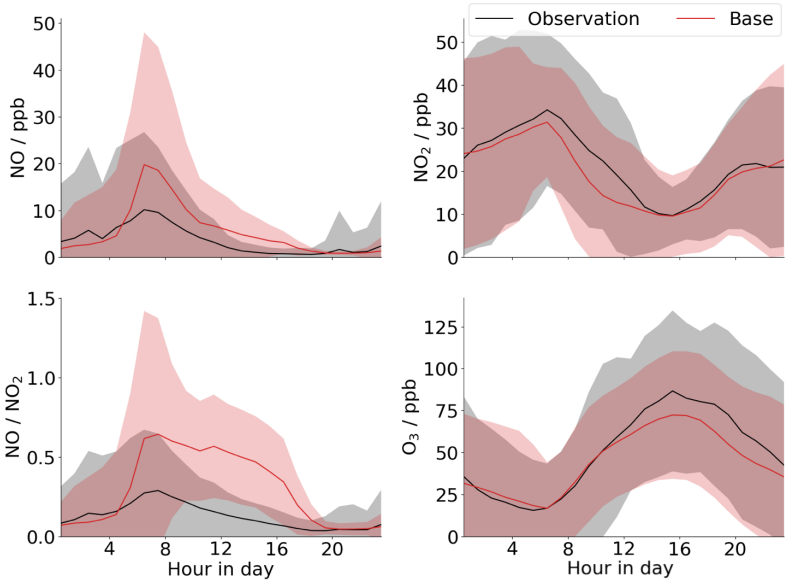

Figure 4: Comparison of GEOS-Chem model output (red) to mean diurnal measurements for the entire campaign (black) for NO, NO_2, O_3 and the NO/NO_2 ratio. Shaded regions are two standard deviations of the mean.

Deleted: for Beijing

Page 42: [1] Deleted	**Mike Newland**	**10/23/20 3:10:00 PM**

Page 42: [1] Deleted	**Mike Newland**	**10/23/20 3:10:00 PM**

Page 42: [1] Deleted	**Mike Newland**	**10/23/20 3:10:00 PM**

Page 42: [1] Deleted	**Mike Newland**	**10/23/20 3:10:00 PM**

Page 42: [1] Deleted	**Mike Newland**	**10/23/20 3:10:00 PM**

Page 42: [1] Deleted	**Mike Newland**	**10/23/20 3:10:00 PM**

Page 42: [1] Deleted	**Mike Newland**	**10/23/20 3:10:00 PM**

Page 42: [2] Deleted	**Mike Newland**	**10/25/20 11:46:00 AM**

Page 42: [2] Deleted	**Mike Newland**	**10/25/20 11:46:00 AM**

Page 42: [2] Deleted	**Mike Newland**	**10/25/20 11:46:00 AM**

Page 42: [2] Deleted	**Mike Newland**	**10/25/20 11:46:00 AM**